An ENU-induced mouse mutant of SHIP1 reveals a critical role of the stem cell isoform for suppression of macrophage activation

Nhu-Y. N. Nguyen,[1,2] Mhairi J. Maxwell,[3] Lisa M. Ooms,[4] Elizabeth M. Davies,[4] Adrienne A. Hilton,[5] Janelle E. Collinge,[5] Douglas J. Hilton,[5] Benjamin T. Kile,[5] Christina A. Mitchell,[4] Margaret L. Hibbs,[3] Stephen M. Jane,[1,2] and David J. Curtis[1,2]

[1]Rotary Bone Marrow Research Laboratories, Royal Melbourne Hospital, Victoria, Australia; [2]Department of Medicine, University of Melbourne, Victoria, Australia; [3]Department of Immunology, Monash University, Victoria, Australia; [4]Department of Biochemistry and Molecular Biology, Monash University, Victoria, Australia; and [5]Molecular Medicine Division, Walter and Eliza Hall Institute of Medical Research, Victoria, Australia

In a recessive ENU mutagenesis screen for embryonic lethality, we identified a mouse pedigree with a missense mutation of SHIP1 (*SHIP1*^{el20}) leading to an amino acid substitution I641T in the inositol-5′-phosphatase domain that represses phosphatidylinositol-3-kinase signaling. Despite detectable expression of functional SHIP1 protein, the phenotype of homozygous *SHIP1*$^{el20/el20}$ mice was more severe than gene-targeted SHIP1-null (*SHIP1*$^{-/-}$) mice. Compared with age-matched *SHIP1*$^{-/-}$ mice, 5-week-old *SHIP1*$^{el20/el20}$ mice had increased myeloid cells, serum IL-6 levels, marked reductions in lymphoid cells, and died by 7 weeks of age with infiltration of the lungs by activated macrophages. Bone marrow transplantation demonstrated that these defects were hematopoietic-cell-autonomous. We show that the el20 mutation reduces expression in *SHIP1*$^{el20/el20}$ macrophages of both SHIP1 and s-SHIP, an isoform of SHIP1 generated by an internal promoter. In contrast, *SHIP1*$^{-/-}$ macrophages express normal levels of s-SHIP. Compound heterozygous mice (*SHIP1*$^{-/el20}$) had the same phenotype as *SHIP1*$^{-/-}$ mice, thus providing genetic proof that the more severe phenotype of *SHIP1*$^{el20/el20}$ mice is probably the result of concomitant loss of SHIP1 and s-SHIP. Our results suggest that s-SHIP synergizes with SHIP1 for suppression of macrophage activation, thus providing the first evidence for a role of s-SHIP in adult hematopoiesis. (*Blood*. 2011; 117(20):5362-5371)

Introduction

Inositol-5′-phosphatases play a critical role in negative regulation of a diverse range of cellular processes, including cell proliferation, survival, and activation. Accordingly, loss of function of these phosphatases is implicated in many disease states, such as autoimmune disease, allergy, and cancer.[1] Germline deletion in the mouse of the hematopoietic-restricted Src homology 2-containing inositol-5′-phosphatase (SHIP1) leads to hyperactive myeloid cells and a shortened life span because of lung infiltration by activated macrophages.[2-4] SHIP1 expression in myeloid cells is particularly important for regulating endotoxin tolerance.[5] Studies of *SHIP1*$^{-/-}$ mice have also demonstrated important roles for SHIP1 in regulating the development and function of B and T cells, mast cells, and basophils.[6-12] However, the analysis of the cellular abnormalities observed in *SHIP1*$^{-/-}$ mice is complicated by the inflammatory response, which can lead to secondary effects, such as loss of B cells through increased production of IL-6.[12,13] Tissue-specific deletion of SHIP1 in macrophages has suggested that loss of B cells in *SHIP1*$^{-/-}$ mice may be secondary to the inflammatory environment.[14,15]

The SHIP1 phosphatase domain inhibits the phosphatidylinositol-3-kinase (PI3K) pathway by hydrolyzing the 5′-phosphate group of the second messenger phosphatidylinositol 3,4,5-trisphosphate (PtdIns(3,4,5)P_3), a lipid that promotes cell survival and proliferation through activation of downstream pleckstrin homology domain-containing enzymes, such as AKT and BTK.[16] Consistent with the 5′-phosphatase function of SHIP1, macrophages and B cells from *SHIP1*$^{-/-}$ mice have increased PI3K signaling as measured by phosphorylation of Akt at Ser^{473}. SHIP1 can also inhibit the Ras/mitogen-activated protein kinase and nuclear factor-κB pathways either by cross-talk with the PI3K pathway or by recruitment of adaptor proteins, such as Shc, Grb2, and Doks to its N-terminal SH2 domain or the C-terminal NPXY motifs and proline-rich regions.[17,18] Both the phosphatase and PI3K-independent activities of SHIP1 may be important for regulation of the inflammatory response.[19,20]

Multiple isoforms of SHIP1 exist, including one identified in embryonic stem cells (s-SHIP) that is transcribed from an internal promoter driving expression in stem and progenitor cells.[21-23] s-SHIP lacks the N-terminal SH2 domain required for binding to Shc but retains the catalytic phosphatase domain and can bind to Grb2, presumably via its C-terminal proline-rich region.[16,21] Importantly, *SHIP1*$^{-/-}$ mice generated by targeting of exon 1 retain expression of s-SHIP; therefore, it has been postulated that s-SHIP expression might moderate the phenotype of *SHIP1*$^{-/-}$ mice.[24,25] However, as yet, a function for s-SHIP in adult hematopoiesis has not been determined.

In an ENU mutagenesis screen, we have identified a point mutant of SHIP1 that results in loss of expression of both SHIP1 and s-SHIP. Mice lacking both SHIP1 and s-SHIP have a severe inflammatory phenotype with macrophage infiltration of the lungs

Submitted January 18, 2011; accepted February 28, 2011. Prepublished online as *Blood* First Edition paper, March 18, 2011; DOI 10.1182/blood-2011-01-331041.

The online version of this article contains a data supplement.

The publication costs of this article were defrayed in part by page charge payment. Therefore, and solely to indicate this fact, this article is hereby marked "advertisement" in accordance with 18 USC section 1734.

and lethality by 7 weeks of age. This provides the first functional evidence that s-SHIP synergizes with SHIP1 for suppression of macrophage activation.

Methods

Gene mapping and mice

A G_3 pedigree with anemia and shortened life span was identified in an ENU mutagenesis screen on a 129Sv background established as previously described.[26] Mapping of the mutation was performed by breeding with wild-type C57BL/6J mice. Genomic DNA was collected from affected and unaffected G_3 mice on weaning and genotyped using a panel of simple sequence-length polymorphism markers. The candidate interval for the mutation was refined to a 3-Mb region of chromosome 1. Subsequent sequencing of candidate genes led to identification of a T to C base substitution at nucleotide position 2099 of the Inpp5 days gene (GenBank Accession NM_010566), which encodes the 5′-phosphatase SHIP1. SHIP1$^{-/-}$ mice were also used and have been described.[12] All mice used for phenotypic analyses were backcrossed onto a C57BL/6J background for at least 5 generations. For repopulation assays, female CD45.1 (B6.SJL(Ptprca[Ly5.1])) mice were purchased from the Walter and Eliza Hall Institute of Medical Research Animal House Facility. The Animal Ethics Committees of the Walter and Eliza Hall Institute and University of Melbourne approved all animal procedures.

Genotyping

SHIP1 point mutant mice were genotyped by an initial polymerase chain reaction (PCR) using primers: forward, (5′-GACCAACTGCTCCTG-GAGAG-3′) and reverse, (5′-TCTGCTTCGTGTATGCATACTTG-3′); followed by a restriction digest of the PCR product with *DpnII* to isolate the T2099C base substitution. *SHIP1*$^{-/-}$ mice were genotyped by 2-allele, 3-primer PCR using primers: forward, (5′-GCCTACGCACTCTGCGTG-3′), reverse, (5′-CTCTGTCCCTGCTCCTGC-3′) and Mk3.3 (5′-GACCG-CTTCCTCGTGCTTTACGGT-3′).

Sample collection and preparation

For flow cytometric analysis, bone marrow cells were harvested by flushing femurs and tibiae with mouse tonicity-phosphate-buffered saline/2% fetal calf serum and running eluant through a 40-μm nylon strainer. Whole organs were filtered through a 40-μm nylon strainer to generate single-cell suspensions. For whole blood counts, 250 μL of blood was collected from the retro-orbital plexus into tubes containing potassium ethylenediaminetetraacetic acid (Sarstedt) and analyzed using an Advia 2120 automated hematologic analyzer (Bayer). For serum analysis, peripheral blood was obtained immediately after death by cardiac puncture and serum prepared using standard procedures. Alveolar macrophages were collected from 4- to 6-week-old mice by bronchoalveolar lavage (BAL). The cellular component of BAL was then lyzed immediately in 100mM NaCl, 10mM Tris-HCl (pH 7.5), 1% glycerol, 2mM ethylenediaminetetraacetic acid, 1% Triton X-100, 0.1% sodium dodecyl sulfate, 50mM NaF, 1mM pervanadate, and Complete protease inhibitors (Roche Diagnostics) for further biochemical studies.

Flow cytometric analysis and sorting

All antibodies used were purchased from BD Biosciences PharMingen or Invitrogen Biosource and were: FITC-conjugated B220 (RA3-6B2), CD8a (53-6.7), CD45.2(104), CD71 (C2/C2F2), IgM (AF6-78), Ly6C (AL-21), and Sca-1 (E13-161-7); phycoerythrin-conjugated B220 (RA3-6B2), CD3 (145-2C11), CD4 (GK1.5), CD19 (1D3), CD45 (30-F11), CD45.1 (A20), c-Kit (ACK45), Ly6G/Gr-1 (1A8), Mac-1a (M1/70), and ter119 (TER-119); BIO-conjugated B220 (RA3-6B2), CD3a (145-2C11), CD8a (53-6.7), CD25 (7D4), Ly6G/Gr-1 (1A8), Mac-1a (M1/70), and ter119 (TER-119); and allophycocyanin-conjugated B220 (RA3-6B2), CD4 (OX-35), and c-Kit (2B8). Second-stage fluorescent reagents used were either SAv-allophycocyanin or SAv-peridinin chlorophyll protein-Cy5.5. The appropriate conjugated rat antimouse isotypes were used as negative controls. Cell viability was determined by exclusion of propidium iodide-positive cells (Sigma-Aldrich). Antibody-labeled cell suspensions were collected on a FACSCalibur flow cytometer (BD Biosciences) or sorted using a FACSVantage SE system (BD Biosciences) and CellQuest software Version 5.2.1 (BD Biosciences). For isolation of lineage$^-$c-Kit$^+$Sca-1$^+$ (LKS) and lineage$^-$c-Kit$^+$Sca-1$^-$ (LK) cell fractions, cell sorting of immature BM cells and immunomagnetic bead depletion of lineage marker$^+$ cells were performed before sorting. All data were analyzed using a Walter and Eliza Hall Institute of Medical Research in-house program, Weasel Version 2.6.2.

Transplantation assays

Bone marrow cells from 3-week-old *SHIP1*$^{+/+}$ and *SHIP1*$^{el20/el20}$ mice were harvested for transplantation by flushing femurs and tibiae with MT-PBS/5% fetal calf serum. Viability of single-cell suspensions was checked by trypan blue exclusion. For competitive transplantations, age- and sex-matched B6.SJL mice (Ly5.1) were used as recipient mice. Recipients were lethally irradiated with 2 doses of 5.5 Gy administered 3 hours apart from a ^{60}Co γ source at a dose rate of 0.45 Gy/minute 2 to 4 hours before transplantation, and transplanted with 2×10^6 donor cells simultaneously with 2×10^6 competitor (Ly5.1) BM cells. A minimum of 3 recipients was used for each donor inoculum. For reciprocal transplantations, 3-week-old *SHIP1*$^{+/+}$ and *SHIP1*$^{el20/el20}$ mice were sublethally irradiated with 2 doses of 3.3 Gy and transplanted with 1.5×10^6 Ly5.1 BM cells. All transplanted mice were fed antibiotic-treated water and housed in hooded cages for the first 3 weeks.

5′-Phosphatase assays

For PtdIns(3,4,5)P_3 5′-phosphatase assays, full-length *SHIP1* and *SHIP1*^{el20} cDNA sequences were subcloned into the pCGN mammalian expression vector in-frame with the N-terminal HA-tag, after which the resultant recombinant plasmids overexpressed in COS-1 cells. Forty-eight hours after transfection, cell lysates were prepared and recombinant proteins immunoprecipitated using HA antibodies (Sigma-Aldrich). 5′-Phosphatase assays were performed on immunoprecipitates as described previously,[27] and parallel immunoprecipitates were immunoblotted with HA antibodies.

Quantitative PCR

Total RNA was extracted from organs, sorted cells, and cultured bone marrow-derived macrophages (BMMΦs) using TRIzol (Invitrogen), and genomic DNA removed using Turbo DNA-free kit (Ambion). Reverse transcription of 1 μg of RNA into cDNA was carried out in 20-μL reactions using the Transcriptor First-strand cDNA Synthesis kit (Roche Diagnostics) with Anchored-oligo(dT)$_{18}$ primers as per the manufacturer's instructions. Quantitative PCR was performed in a LightCycler 480 II (Roche Diagnostics) using 10 μL of 2× SYBR Green PCR Master Mix (Applied Biosystems), 1 μL of 10μM specific primers, and 1 μL of cDNA. Primer sequences used were as follows: hypoxanthine phosphoribosyl transferase (HPRT): forward, 5′-GCTGGTGAAAAGGACCTCT-3′; reverse, 5′-CACAG-GACTAGAACACCTGC-3′ (248 bp); SHIP1: forward, 5′-GGCTCCAGCAAC-CTCCCTCAC-3′; reverse, 5′-TTCTCC GTCTCCACCAAAATCACC-3′ (491 bp); and s-SHIP: forward, 5′-GTTCCCACTAGATGTTGA ACTTTAC-3′; reverse, 5′-TCTCCTTCTCCGTCTCCACC-3′ (442 bp). For HPRT, amplification was performed at 95°C for 5 minutes, followed by 40 cycles of 15 seconds at 94°C, 30 seconds at 60°C, and 30 seconds at 82°C. For SHIP1 and s-SHIP, touchdown amplification was performed at 94°C for 5 minutes, followed by 43 cycles of 15 seconds at 94°C, 30 seconds at 62°C to 42°C (decreasing by 0.5°C/cycle) and 30 seconds at 72°C. All results were normalized to HPRT and expressed as relative gene expression for each target gene.

Histologic analysis

Whole lungs were fixed in 10% neutral buffered formalin and embedded in paraffin for sectioning. Sections were prepared and stained with hematoxylin and eosin at the Walter and Eliza Hall Institute. Images were acquired

using a Nikon Eclipse 80i; microscope equipped with a 40×/0.75 NA objective lens. Images were captured with a Nikon XM1200C digital camera, and figures were created using Adobe Photoshop CS4, Version 11.0.1 (Adobe Systems Inc).

IL-6 ELISA

Serum samples and tissue culture supernatants of resting or stimulated BMMΦs were assessed for protein levels of IL-6 by ELISA (BD Biosciences) according to the manufacturer's instructions.

Tissue culture

To obtain BMMΦs, bone marrow cells were sterilely collected from femurs and tibiae of 4- to 6-week-old mice and allowed to adhere overnight at 37°C, 5% CO_2 in BMMΦ medium (DMEM + 15% fetal calf serum + penicillin/streptomycin + 20% L cell conditioned medium [as a source of macrophage colony stimulating factor]). Nonadherent cells were then transferred to fresh tissue culture plates and incubated at 37°C, 5% CO_2 for 5 days in BMMΦ medium with the addition of 10% volume L cell conditioned medium every second day.

LPS treatments

For IL-6 analysis, BMMΦs at 1×10^6 cells/mL were serum-starved overnight then incubated with 100 ng/mL lipopolysaccharide (LPS) for various time points before supernatants harvested and used for ELISA.

Western blots

Whole cell lysates of resting BMMΦs were prepared by solubilization in lysis buffer containing 10mM N-2-hydroxyethylpiperazine-N′-2-ethanesulfonic acid (pH 7.6), 250mM Nonidet P-40, 5mM ethylenediaminetetraacetic acid, and Complete protease inhibitors (Roche Diagnostics) for 1 hour on ice. Lysates were clarified by centrifugation at 13 000*g* for 20 minutes at 4°C and protein levels determined by Bradford assay. Lysates were boiled for 5 minutes and then fractionated by SDS-PAGE electrophoresis before being transferred onto Hybond-P polyvinylidene difluoride or nitrocellulose membranes (GE Healthcare). Immunoblotting for specific primary antibodies was performed as per the manufacturer's instructions and with the appropriate horseradish peroxidase-conjugated secondary antibody (GE Healthcare). Protein levels were detected using an ECL kit (GE Healthcare). Antibodies against the following were used: SHIP1 and tubulin (Santa Cruz Biotechnology); and Akt, phospho-Akt (Ser^{473}), S6, and phospho-pS6 (Cell Signaling Technologies). In experiments assessing the phosphorylation state of proteins in alveolar macrophages, blots were analyzed using the Odyssey Infrared Imaging System and fluorescence-conjugated secondary antibodies (LI-COR Biosciences), and the fluorescence signal converted to grayscale for figures using Odyssey Application software Version 2.0.

Results

Generation of a SHIP1 mutant mouse by ENU mutagenesis

In a recessive ENU mouse mutagenesis screen established to identify mutants with early lethality,[26] we identified a G_3 pedigree (el20) with runting and pancytopenia. The mutation was mapped to a 3-Mb region on chromosome 1, and sequencing of candidate genes led to identification of a T to C base substitution at nucleotide position 2099 of *Inpp5d*. The *Inpp5d* locus encodes the inositol 5′-phosphatase SHIP1, and the point mutation is predicted to cause an amino acid substitution of an evolutionarily conserved isoleucine residue to threonine at amino acid position 641 (Figure 1A). This mutant allele is referred to as $SHIP1^{el20}$. The change from a hydrophobic to hydrophilic residue located within the α7-β9 loop region of the SHIP1 catalytic 5′-phosphatase domain was predicted to alter enzymatic activity. An in vitro 5′-phosphatase assay demonstrated that this mutant showed enzyme activity, but this was reduced compared with wild-type SHIP1 protein, which hydrolyzed all PtdIns(3,4,5)P_3 present to form PtdIns(3,4)P_2 (Figure 1B). Western blot analyses of cell lysates generated from homozygous mutant ($SHIP1^{el20/el20}$) BMMΦs demonstrated less than 10% of the normal SHIP1 protein levels (Figure 1C). This reduced protein expression could be explained by reduced mRNA levels as determined by quantitative real-time PCR of cDNA isolated from whole bone marrow, thymus, freshly isolated LK progenitors and cultured BMMΦs (Figure 1D). Thus, the $SHIP1^{el20}$ mutation led to markedly reduced levels of SHIP1 protein, presumably because of the mutation affecting RNA stability.

$SHIP1^{el20/el20}$ mice exhibit failure to thrive and early lung disease

Heterozygous mutant mice ($SHIP1^{+/el20}$) displayed no significant abnormalities when examined up to 12 months of age (data not shown). At weaning, homozygous $SHIP1^{el20/el20}$ mice were present at expected Mendelian ratios but exhibited runting and a subsequent failure to thrive (Figure 2A-B). Survival of $SHIP1^{el20/el20}$ mice was significantly impaired, with no mutant mice living beyond 7 weeks of age compared with 50% survival of SHIP1-null ($SHIP1^{-/-}$) mice at 6 months of age (Figure 2C). These differences in survival could not be attributed to differences in genetic background or the environment as both $SHIP1^{el20/el20}$ mice and $SHIP1^{-/-}$ mice were maintained on a C57BL/6 background in similar housing conditions. Death of $SHIP1^{-/-}$ mice is the result of respiratory failure from alveoli filled with lipid-laden macrophages containing eosinophilic Ym1 crystals, a product of activated macrophages.[2,3] Histologic examination of lungs from 4-week-old $SHIP1^{el20/el20}$ mice revealed severe lung pathology similar to that reported in older $SHIP1^{-/-}$ mice (Figure 2D). As expected, lungs of 4-week-old $SHIP1^{-/-}$ mice were relatively unaffected. Thus, the significantly shorter survival of $SHIP1^{el20/el20}$ mice appears to be explained by a more rapid onset of respiratory failure from accumulation of activated macrophages in the lungs.

$SHIP1^{el20/el20}$ mice have more marked hematopoietic abnormalities than $SHIP1^{-/-}$ mice

Given that $SHIP1^{el20/el20}$ mice express detectable levels of SHIP1 protein, albeit with reduced catalytic activity (Figure 1B-C), the more dramatic lung phenotype was surprising. We analyzed hematopoiesis in $SHIP1^{el20/el20}$ mice at 4 to 5 weeks of age, a time point before the development of major systemic illness, to determine whether the hematopoietic phenotype was also more severe than age-matched $SHIP1^{-/-}$ mice. Peripheral blood analysis of 5-week-old $SHIP1^{el20/el20}$ mice demonstrated significantly reduced numbers of circulating lymphocytes compared with age-matched $SHIP1^{-/-}$ mice (Table 1). $SHIP1^{el20/el20}$ mice also displayed anemia and thrombocytopenia, but these abnormalities were of similar severity to $SHIP1^{-/-}$ mice (Table 1).

The bone marrow cellularity of $SHIP1^{el20/el20}$ mice was significantly reduced because of a marked (50-fold) reduction of pre-B cells ($B220^{lo}CD25^{+}$) and mature B cells (Table 1; Figure 3A). A similar, but less severe, reduction of B cells was observed in the BM of older (10-week) $SHIP1^{-/-}$ mice (supplemental Table 1, available on the *Blood* Web site; see the Supplemental Materials link at the top of the online article). Consistent with a negative regulatory role for SHIP1 in B-cell antigen receptor signaling,[28] $SHIP1^{el20/el20}$ mice had a 53-fold increase in serum IgM levels

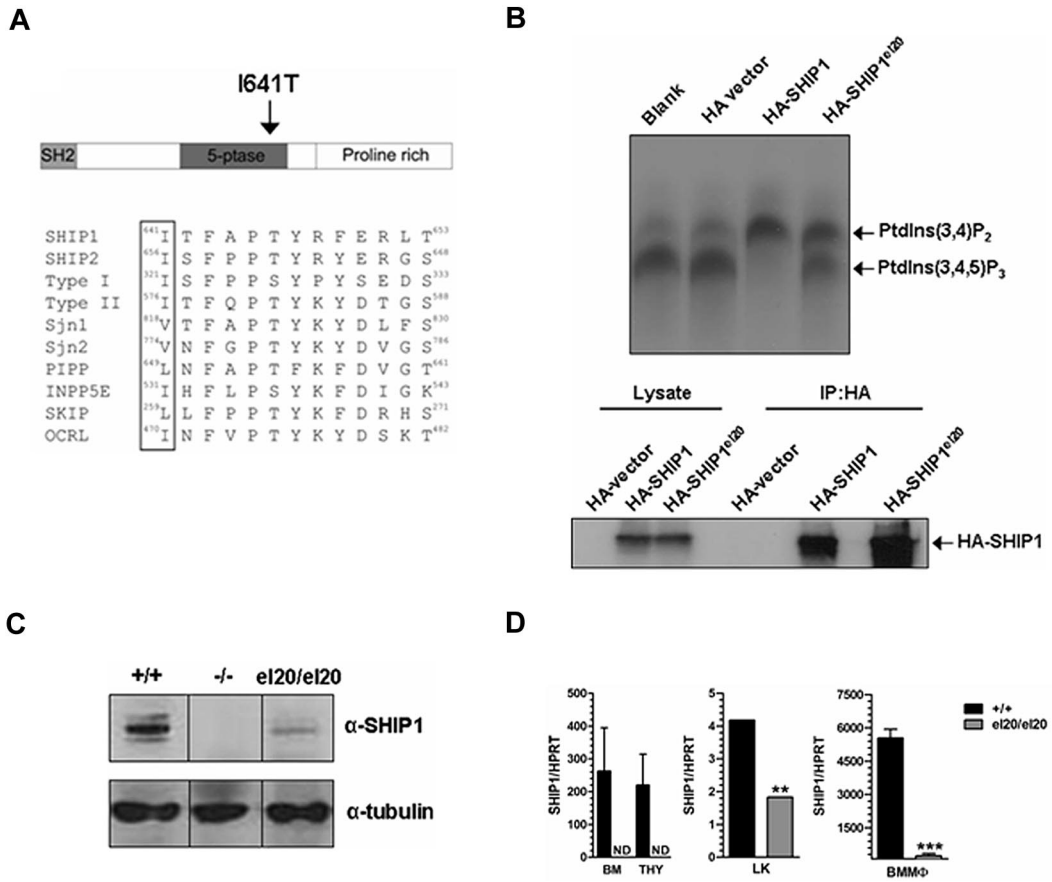

Figure 1. Identification of a missense point mutation of *SHIP1*. (A) Schematic of the isoleucine to threonine amino acid substitution in the 5′-phosphatase domain of SHIP1 and the corresponding conserved hydrophobic residue of other inositol 5′-phosphatases. (B) 5′-Phosphatase assay showing the conversion of PtdIns(3,4,5)P_3 substrate to PtdIns(3,4)P_2 product by immunoprecipitated recombinant wild-type or mutant SHIP1. The HA vector sample is included as a transfection control, and results are representative of 2 individual experiments. The HA-immunoblot of lysates and parallel HA-immunoprecipitates, on which the 5′-phosphatase assays were performed, demonstrates similar loading of SHIP1 protein. (C) Western blot for SHIP1 expression in resting *SHIP1*$^{+/+}$, *SHIP1*$^{-/-}$, and *SHIP1*$^{el20/el20}$ BMMΦs. Western blot is representative of 3 independent samples for each genotype. (D) Quantitative RT-PCR for SHIP1 mRNA expression in whole bone marrow (BM), thymus (THY), sorted lineage$^-$c-Kit$^+$ (LK) BM cells and resting BMMΦs. All values have been normalized to expression of HPRT. Bar graphs represent the mean ± SD of 3 samples for each genotype, with the exception of LK cells, which were obtained from sorts of 3 mice for each genotype. $^{**}P < .01$, 2-tailed Mann-Whitney test. $^{***}P < .001$, 2-tailed Mann-Whitney test. ND indicates not detected.

(supplemental Figure 1A). Levels of serum IgG were not significantly altered, although there was a trend toward increased IgG_{2a} (supplemental Figure 1B), which has been reported in *SHIP1*$^{-/-}$ mice.[29] Consistent with a role for SHIP1 in the repression of myeloid immunoregulatory macrophages,[8] *SHIP1*$^{el20/el20}$ mice displayed a 3-fold increase in the numbers of Mac-1$^+$Gr-1$^+$ cells within the BM (Table 1; Figure 3B). *SHIP1*$^{el20/el20}$ mice also had increased spleen size because of markedly increased erythropoiesis and, to a lesser extent, Mac-1$^+$Gr-1$^+$ cells (Table 1).

In addition to the marked B-cell deficiency, *SHIP1*$^{el20/el20}$ mice also exhibited very small thymi (10- to 20-fold smaller than controls), affecting all T-cell subsets but most notably the CD4$^+$CD8$^+$ double-positive (DP) fraction (Table 1; Figure 3C). In contrast, *SHIP1*$^{-/-}$ mice had normal numbers of thymocytes, even at 10 weeks of age (supplemental Table 1).

Cell-autonomous and non–cell-autonomous hematopoietic defects of *SHIP1*$^{el20/el20}$ mice

SHIP1 expression is predominantly hematopoietic, although expression has also been demonstrated in the testis, fibroblasts, endothelial cells, and osteoblasts.[30-32] We transplanted BM cells from *SHIP1*$^{el20/el20}$ mice into lethally irradiated wild-type mice to determine whether the more severe phenotype, including impaired survival of *SHIP1*$^{el20/el20}$ mice, was intrinsic to the hematopoietic cells. Within 6 weeks of transplantation, mice reconstituted with *SHIP1*$^{el20/el20}$ BM exhibited hallmarks of the *SHIP1*$^{el20/el20}$ phenotype, including splenomegaly and reduced DP thymocytes (supplemental Figure 2) with death of most mice within 12 weeks of transplantation because of macrophage infiltration of the lungs. The phenotype was not as rapid or severe as that observed in *SHIP1*$^{el20/el20}$ mice, which may be explained by the slower kinetics of tissue macrophage turnover, especially in the lungs.[33] Conversely, transplantation of wild-type BM cells into 3-week-old *SHIP1*$^{el20/el20}$ mice rescued the hematopoietic phenotype (supplemental Figure 2) and their survival, with the majority of mice surviving beyond 12 weeks after transplantation. A small number of *SHIP1*$^{el20/el20}$ mice died, but analysis revealed expansion of endogenous *SHIP1*$^{el20/el20}$ BM cells surviving the irradiation (data not shown). Thus, the hematopoietic defects and impaired survival of *SHIP1*$^{el20/el20}$ mice were hematopoietic cell-autonomous.

The role of SHIP1 in hematopoietic stem cell (HSC) function is complex, with reports of either normal or increased activity in *SHIP1*$^{-/-}$ mice.[30,31,34] We performed competitive BM transplantation assays to evaluate the effect of the *SHIP1*^{el20} mutation on HSC function. Donor CD45.2$^+$ BM cells from wild-type or *SHIP1*$^{el20/el20}$

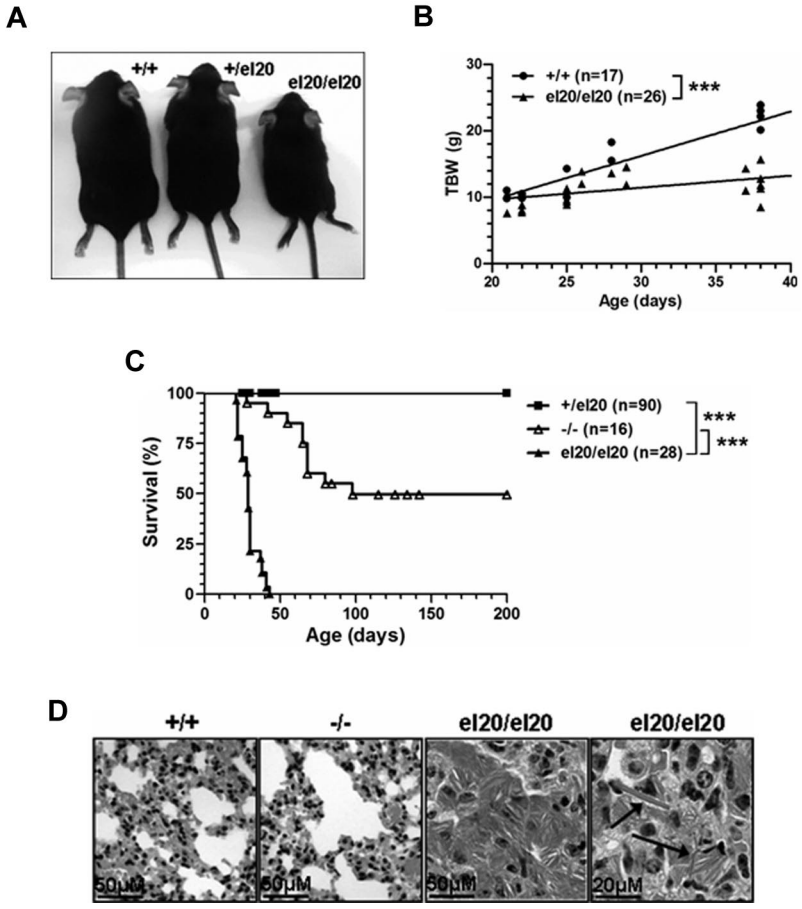

Figure 2. Homozygous *SHIP1*$^{el20/el20}$ mice have runting, early lethality, and severe lung disease. (A) Five-week-old sex-matched littermates showing runting of a homozygous *SHIP1*$^{el20/el20}$ mouse compared with wild-type *SHIP1*$^{+/+}$ and heterozygous *SHIP1*$^{+/el20}$ mice. (B) Total body weight (TBW) of male *SHIP1*$^{el20/el20}$ mice compared with male *SHIP1*$^{+/+}$ controls. ***$P < .001$ using 1-way ANOVA. (C) Survival curves of *SHIP1*$^{el20/el20}$ mice compared with *SHIP1*$^{-/-}$ and *SHIP1*$^{+/el20}$ mice. ***$P < .0001$ using log-rank (Mantel Cox) test. (D) Hematoxylin and eosin–stained histologic lung sections of 4-week-old *SHIP1*$^{el20/el20}$ mice showing alveolar airspace consolidation of lungs with macrophages containing eosinophilic Ym1 crystals (arrows). Normal lungs from age-matched *SHIP1*$^{+/+}$ and *SHIP1*$^{-/-}$ mice are shown.

mice were transplanted with equal numbers of wild-type competitor CD45.1$^+$ BM cells into lethally irradiated CD45.1$^+$ wild-type mice. Evaluation of the proportions of donor and competitor hematopoietic cells in the peripheral blood (Figure 4A) and hematopoietic organs (Figure 4B) demonstrated similar contributions by donor wild-type and *SHIP1*$^{el20/el20}$ HSCs, indicating that the *SHIP1*^{el20} mutation had no significant effect on HSC activity. However, mice receiving *SHIP1*$^{el20/el20}$ donor BM cells exhibited significantly reduced thymus size and numbers of BM pre-B cells because of loss of both donor *SHIP1*$^{el20/el20}$ and wild-type competitor cells (Figure 4C). This suggested that the lymphoid defects in *SHIP1*$^{el20/el20}$ mice are mediated in part by a non–cell-autonomous mechanism.

SHIP1$^{el20/el20}$ macrophages have increased IL-6 production

Elevated levels of circulating IL-6 secreted by activated macrophages are a proposed non–cell-autonomous mechanism of reduced B-cell numbers in *SHIP1*$^{-/-}$ mice.[13,35] Therefore, we measured serum IL-6 levels in age-matched *SHIP1*$^{el20/el20}$ and *SHIP1*$^{-/-}$ mice. Serum IL-6 levels in 4- to 5-week-old *SHIP1*$^{el20/el20}$ mice were 100-fold greater than in control mice and 3-fold greater than in age-matched *SHIP1*$^{-/-}$ mice (Figure 5A). We examined IL-6 production by BMMΦs to address a potential source of the elevated serum IL-6. *SHIP1*$^{el20/el20}$ macrophages displayed markedly elevated basal levels of IL-6 compared with control BMMΦs (Figure 5B). Secretion of IL-6 by resting *SHIP1*$^{-/-}$ macrophages was not increased, consistent with the recent finding that peritoneal and splenic macrophages are the major source of IL-6 in *SHIP1*$^{-/-}$ mice.[36] SHIP1 has also been implicated in the LPS response, although reports of its effects on IL-6 production by BMMΦs are conflicting.[5,37] In our hands, *SHIP1*$^{-/-}$ BMMΦs had a blunted IL-6 response to LPS at the 3-hour time point as previously reported.[5,37] In contrast, *SHIP1*$^{el20/el20}$ BMMΦs had a normal LPS response (Figure 5C). Thus, cultured *SHIP1*$^{el20/el20}$ macrophages had increased LPS response compared with *SHIP1*$^{-/-}$ macrophages, consistent with the increased serum IL-6 levels and the more severe lung inflammatory phenotype of *SHIP1*$^{el20/el20}$ mice.

We next investigated the effect of the *SHIP1*^{el20} mutation on the PI3K/mammalian target of rapamycin signaling cascade. After a 5-hour serum starvation, *SHIP1*$^{el20/el20}$ BMMΦs had mildly increased pAkt relative to wild-type, although not significantly greater than that seen in *SHIP1*$^{-/-}$ BMMΦs (Figure 5D). pAkt was similar to wild-type in freshly isolated BAL cells obtained from 5-week-old *SHIP1*$^{el20/el20}$ and 10-week-old *SHIP1*$^{-/-}$ mice (Figure 5E). In contrast to minimal changes in pAkt levels, there was marked increase in total S6 and pS6, a downstream target of the mTORC1 complex (Figure 5F). Thus, the SHIP1^{el20} mutation leads to activation of the PI3K/mTOR pathway as measured by pS6, although not different from that observed in *SHIP1*$^{-/-}$ BAL cells.

Table 1. Hematopoietic cell numbers in *SHIP1*$^{el20/el20}$ mice

	SHIP1$^{+/+}$	*SHIP1*$^{el20/el20}$	*SHIP1*$^{-/-}$
Peripheral blood			
Hematocrit, %	44.7 ± 1.0	40.5 ± 1.1*	39.6 ± 4.2*
White cells, × 10^9/L	10.9 ± 0.8	7.2 ± 0.2*†	9.9 ± 0.7
Lymphocytes, × 10^9/L	8.8 ± 0.6	5.1 ± 0.2*†	7.2 ± 0.6
Neutrophils, × 10^9/L	1.5 ± 0.1	1.6 ± 0.1	1.7 ± 0.4
Platelets, × 10^9/L	1016 ± 81	499 ± 52*	607 ± 78*
Bone marrow, cells × 10^6	61 ± 4	49 ± 5*†	71 ± 5
Pre-B	9.4 ± 1.7	0.2 ± 0.1*†	9.0 ± 0.2
Mature B	2.5 ± 0.9	0.2 ± 0.1*†	2.8 ± 0.2
Mac-1$^+$	18 ± 0.4	23 ± 3.6	22 ± 1.4*
Mac-1$^+$Gr-1$^+$	7.3 ± 0.8	21 ± 2.3*	NA
Pro-erythroblast	23 ± 1.6	20 ± 4.8	23 ± 2.3
Late erythroblast	10 ± 1.2	5.7 ± 0.7*	15 ± 0.4*
Spleen, cells × 10^6	107 ± 8	224 ± 4*†	98 ± 14
B220$^+$	17 ± 5	9 ± 3†	23 ± 3
CD4$^+$	12 ± 3	6 ± 1*	9 ± 1
CD8$^+$	7 ± 1	4 ± 1*	5 ± 1
Mac-1$^+$	18 ± 4	23 ± 01	14 ± 6
Mac-1$^+$Gr-1$^+$	16 ± 2	22 ± 2*	NA
Pro-erythroblast	9 ± 2	143 ± 26*†	14 ± 2*
Late erythroblast	24 ± 4	28 ± 0.7	19 ± 1
Thymus, cells × 10^6	91 ± 13	6.5 ± 2.7*	103 ± 3
DN	3.1 ± 0.6	1.4 ± 0.7*†	3.1 ± 0.3
DP	76 ± 12	2.7 ± 0.7*†	80 ± 10
CD4$^+$	8.4 ± 1.4	1.7 ± 0.3*†	8.9 ± 1.1
CD8$^+$	2.8 ± 0.5	0.7 ± 0.2*†	4.5 ± 0.5*

Analyses of peripheral blood and hematopoietic organs were performed on 5-week-old *SHIP1*$^{+/+}$, *SHIP1*$^{-/-}$, and *SHIP1*$^{el20/el20}$ mice. Values are the mean ± SD of at least 3 mice for each genotype. BM cell numbers were calculated per femur.

Pre-B indicates B220^{lo}CD25$^+$; mature B, B220^{hi}IgM$^+$; Pro-erythroblast, ter119$^+$CD71^{hi}; Late erythroblast, ter119$^+$CD71$^-$; and NA, not assessed.

*$P < .05$ by 2-tailed Mann-Whitney test versus *SHIP1*$^{+/+}$ controls.

†$P < .05$ by 2-tailed Mann-Whitney test versus *SHIP1*$^{-/-}$ mice.

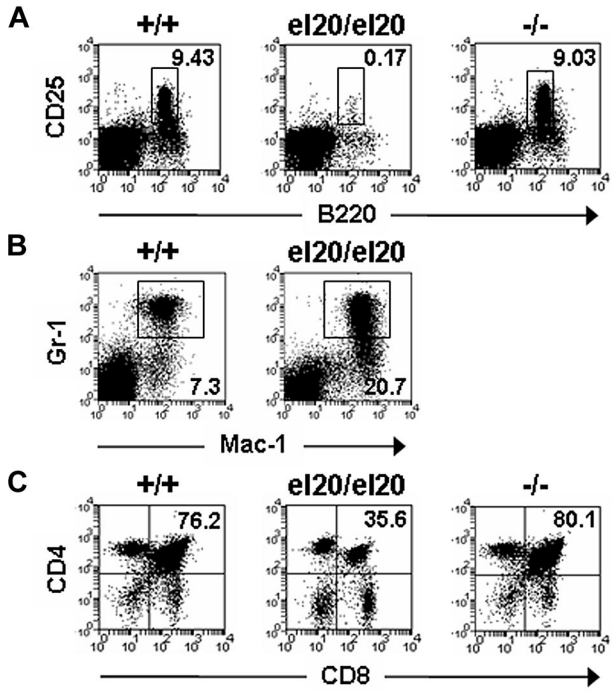

Figure 3. Hematopoietic defects of *SHIP1*$^{el20/el20}$ mice. Representative dot plots of (A) bone marrow B220^{lo}CD25$^+$ pre-B cells, (B) bone marrow Mac-1$^+$Gr-1$^+$ myeloid cells, and (C) thymic T-cell subsets from 5-week-old mice. The mean proportion for each subset was gated on live hematopoietic cells and calculated from at least 3 mice of each genotype.

The more severe inflammatory phenotype of *SHIP1*$^{el20/el20}$ mice is the result of loss of both SHIP1 and s-SHIP

Gene targeting of exon 1 of the *Inpp5d* locus does not prevent expression of the shorter s-SHIP isoform, which is initiated from an alternate promoter within intron 5.[21] Although s-SHIP expression is reported to be limited to embryonic stem cells and HSCs, s-SHIP mRNA was detectable in lineage-restricted hematopoietic cells, including Mac-1$^+$ myeloid cells at levels comparable with embryonic stem cells (Figure 6A). We examined s-SHIP mRNA expression in BMMΦs generated from wild-type *SHIP1*$^{+/+}$, *SHIP1*$^{-/-}$, and *SHIP1*$^{el20/el20}$ mice to determine whether s-SHIP expression was affected by the *SHIP1*^{el20} mutation (Figure 6B). As predicted by the targeting strategy used to generate the *SHIP1*$^{-/-}$ mice, s-SHIP mRNA was expressed at normal levels in *SHIP1*$^{-/-}$ macrophages. In contrast, *SHIP1*$^{el20/el20}$ macrophages expressed 20-fold less s-SHIP mRNA. Thus, the *SHIP1*^{el20} mutation leads to loss of both SHIP1 and s-SHIP mRNA expression in macrophages.

We hypothesized that the more dramatic phenotype of *SHIP1*$^{el20/el20}$ mice was the result of concomitant loss of SHIP1 and s-SHIP expression. To address this hypothesis, we crossed heterozygous *SHIP1*$^{+/-}$ mice with heterozygous *SHIP1*$^{+/el20}$ mice to generate compound heterozygous *SHIP1*$^{-/el20}$ mice, which should express a single allele of *s-SHIP* from the *SHIP1*$^-$ targeted locus. Quantitative real-time PCR confirmed expression of s-SHIP in compound heterozygous *SHIP1*$^{-/el20}$ BMMΦs (Figure 6B). Examination of *SHIP1*$^{-/el20}$ mice at 6 weeks of age revealed complete rescue of the pre-B-cell and thymocyte phenotype (Figure 6C). In addition, serum IL-6 levels and IL-6 production by BMMΦs were

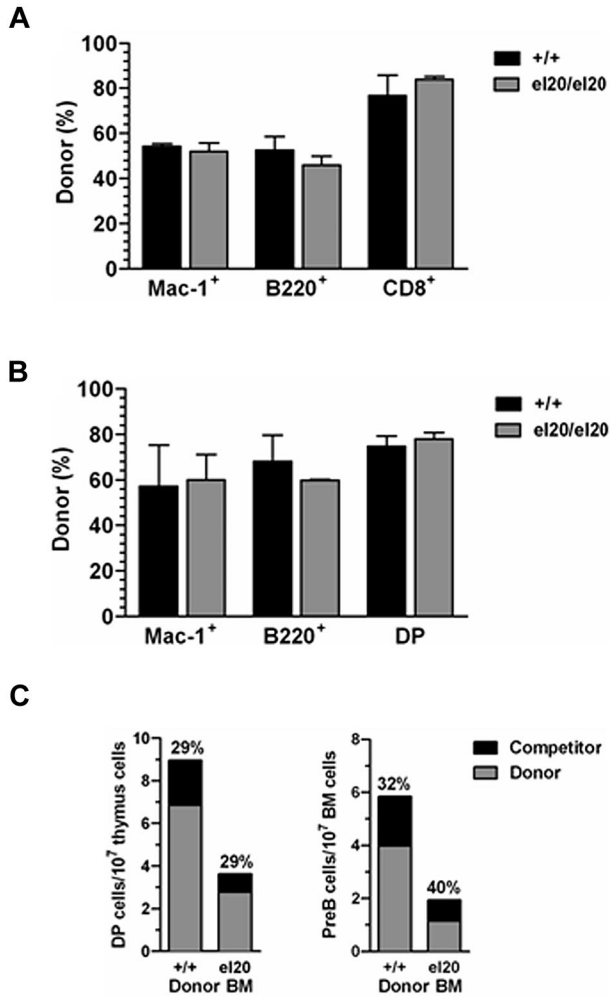

Figure 4. Reduced number of lymphoid cells in *SHIP1*$^{el20/el20}$ mice is non–cell-autonomous. (A) Donor contribution of myeloid (Mac-1$^+$), B-cell (B220$^+$), and T-cell (CD8$^+$) lineages in peripheral blood of recipient mice 4 weeks after transplantation with a 1:1 ratio of donor (*SHIP1*$^{+/+}$ or *SHIP1*$^{el20/el20}$) and wild-type CD45.1 competitor BM cells. Bar graphs represent the mean ± SD calculated from 3 recipients of each donor genotype. (B) Donor contribution 12 weeks after transplantation. Mice were killed to determine donor contribution to the BM myeloid (Mac-1$^+$), BM B-cell (B220$^+$), and thymic T-cell (DP) lineages. Bar graphs represent the mean ± SD calculated from 3 recipients of each donor genotype. (C) Total numbers of DP thymocytes and pre-B cells in mice 12 weeks after transplantation with a 1:1 ratio of donor (*SHIP1*$^{+/+}$ or *SHIP1*$^{el20/el20}$) and wild-type CD45.1 competitor BM cells. The relative contribution of competitor cells is shown.

restored to that observed in *SHIP1*$^{-/-}$ mice and BMMΦs, respectively (Figure 6D-E). Histologic examination of the lungs from *SHIP1*$^{-/el20}$ mice was also normal at 6 weeks of age but, similar to *SHIP1*$^{-/-}$ mice, showed evidence of abnormal macrophage deposition by 11 weeks of age (Figure 6F). Most importantly, *SHIP1*$^{-/el20}$ mice had a similar survival to *SHIP1*$^{-/-}$ mice (Figure 6G). Thus, the *SHIP1*$^-$ targeted locus, which expresses *s-SHIP*, was able to restore the more dramatic phenotype of *SHIP1*$^{el20/el20}$ mice back to the *SHIP1*$^{-/-}$ phenotype.

Discussion

We present the phenotype of a point mutant of SHIP1 resulting from ENU mutagenesis. Although the phenotype of *SHIP1*$^{el20/el20}$ mice was similar to *SHIP1*$^{-/-}$ mice, it was much more dramatic with early lethality (death by 7 weeks of age) associated with marked macrophage infiltration of the lungs and marked reductions of pre-B cells and thymocytes. We provide several pieces of evidence that the accentuated phenotype was the result of loss of expression of s-SHIP, an isoform of SHIP1 with no previously known function. First, we show that s-SHIP mRNA is expressed in mature hematopoietic cells at levels comparable with embryonic stem cells despite previous reports that it is stem cell-restricted.[21,22]

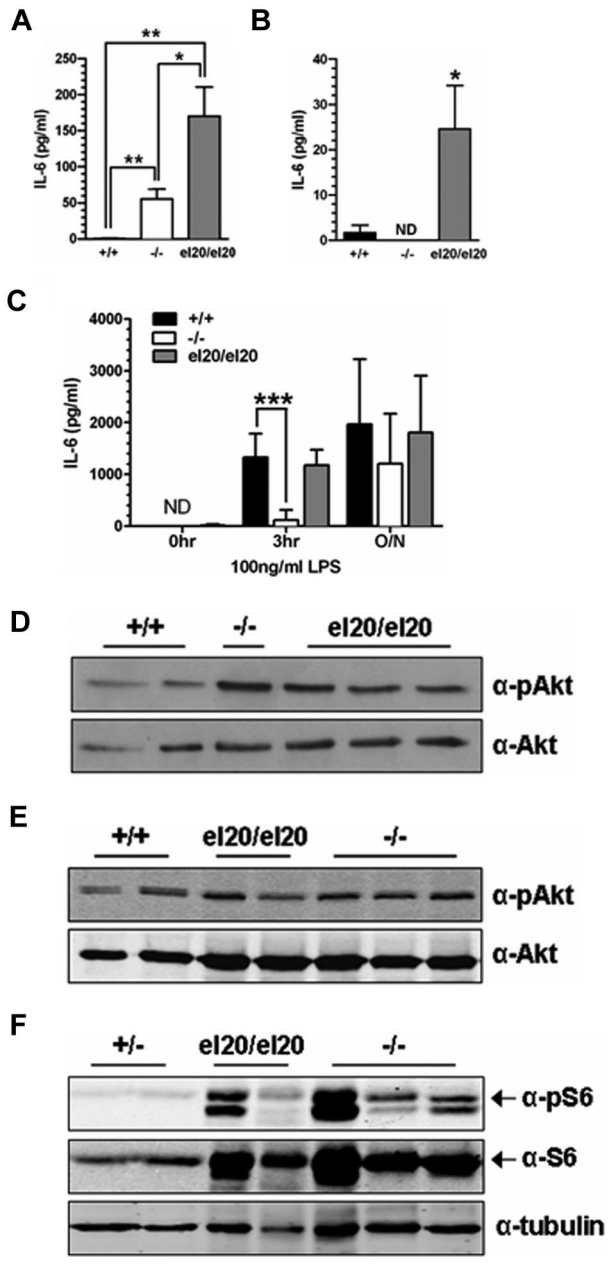

Figure 5. Increased IL-6 production and PI3K/mTOR signaling in *SHIP1*$^{el20/el20}$ mice. (A) IL-6 levels in serum from 4- to 5-week-old mice. Bar graph represents the mean ± SD of at least 3 mice for each genotype. *$P < .05$, 2-tailed Mann-Whitney test. **$P < .01$, 2-tailed Mann-Whitney test. (B) IL-6 levels in resting BMMΦs. Bar graph represents the mean ± SD of at least 6 samples for each genotype. *$P < .05$, 2-tailed Mann-Whitney test compared with *SHIP1*$^{+/+}$ control. ND indicates not detected. (C) IL-6 levels in resting BMMΦs after stimulation with LPS for the indicated times. Bar graph represents the mean ± SD of 6 independent samples for each genotype. ***$P < .001$, 2-tailed Mann-Whitney test compared with *SHIP1*$^{+/+}$ control. ND indicates not detected. (D) Western blot for pAkt Ser^{473} and total Akt in resting BMMΦs. (E) Western blot for pAkt Ser^{473} and total Akt in freshly isolated BAL cells from the same mice used for panel D. (F) Western blot for pS6 and total S6 in freshly isolated BAL cells from the same mice used for panel D except for the controls, which were from *SHIP1*$^{+/-}$ heterozygous mice.

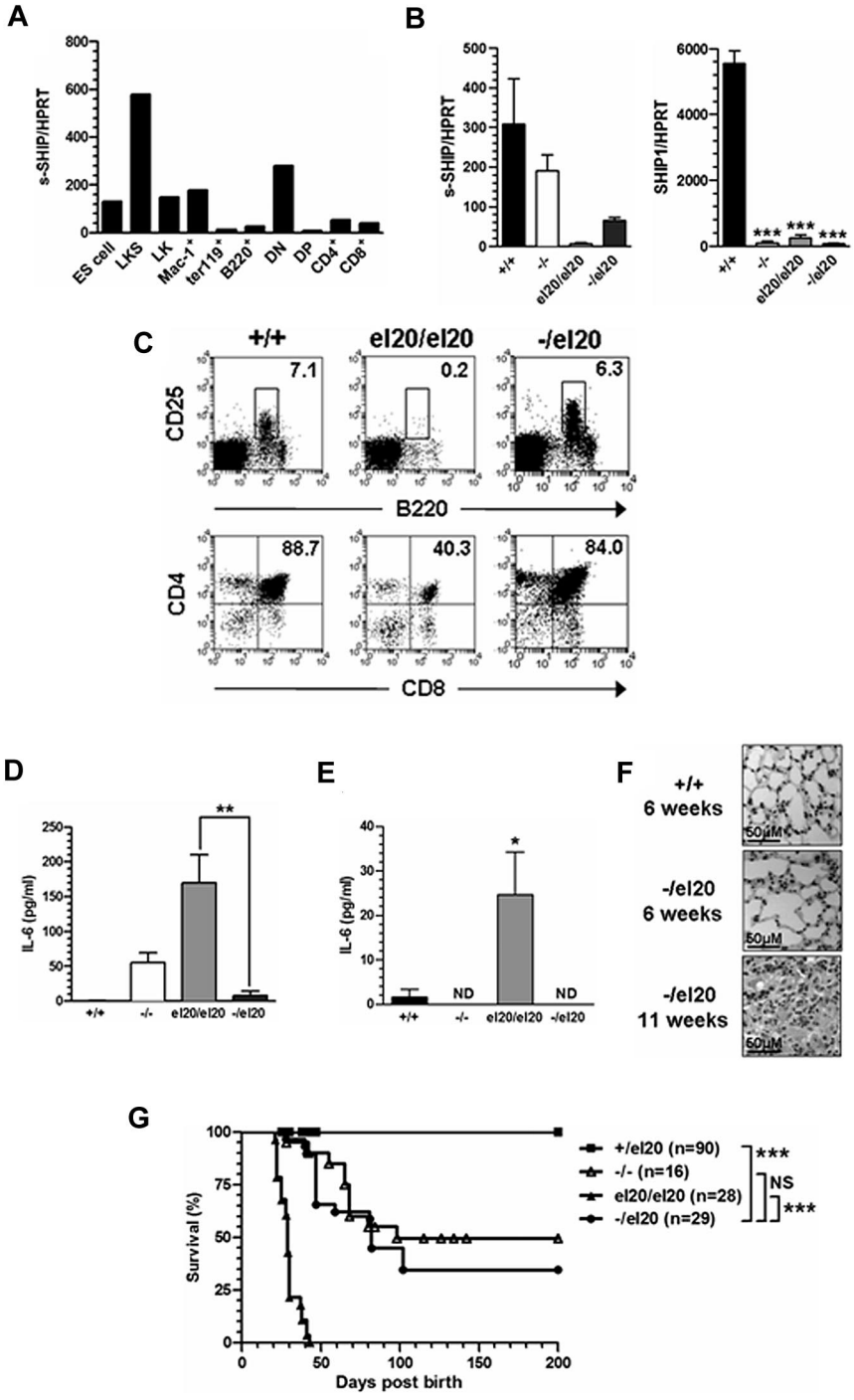

Figure 6. The el20 mutation leads to loss of expression of both SHIP1 and the s-SHIP isoform. (A) Quantitative RT-PCR for s-SHIP mRNA expression in wild-type sorted hematopoietic cell subsets. Sorted cell subsets were obtained from pools of at least 3 mice. All values have been normalized to expression of HPRT. LKS indicates lineage$^-$c-Kit$^+$Sca-1$^+$; LK, lineage$^-$c-Kit$^+$; DN, CD4$^-$CD8$^-$ double-negative thymocytes; and DP, CD4$^+$CD8$^+$ double-positive thymocytes. (B) Quantitative RT-PCR for s-SHIP and SHIP1 mRNA expression in BMMΦs from wild-type *SHIP1*$^{+/+}$, *SHIP1*$^{-/-}$, *SHIP1*$^{el20/el20}$, and compound heterozygous *SHIP1*$^{-/el20}$ mice. All values have been normalized to expression of HPRT. Bar graphs represent the mean ± SD of 4 samples for each genotype. ***$P < .0001$ using log-rank (Mantel Cox) test compared with *SHIP1*$^{+/+}$ control. (C) Representative dot plots of bone marrow pre-B cells (top panel) and thymic T-cell subsets (bottom panel). The mean proportion for each subset was gated on live hematopoietic cells and calculated from at least 3 mice of each genotype. (D) IL-6 levels in serum of age-matched *SHIP1*$^{-/el20}$ mice compared with *SHIP1*$^{+/+}$, *SHIP1*$^{-/-}$, and *SHIP1*$^{el20/el20}$ mice shown in Figure 5A. **$P < .01$ by 2-tailed Mann-Whitney test. (E) IL-6 production by resting *SHIP1*$^{-/el20}$ BMMΦs compared with *SHIP1*$^{+/+}$, *SHIP1*$^{-/-}$, and *SHIP1*$^{el20/el20}$ samples shown in Figure 5B. *$P < .05$, 2-tailed Mann-Whitney test. ND indicates not detected. (F) Hematoxylin and eosin-stained histologic sections showing normal lungs at 6 weeks of age but consolidation of alveolar airspaces in 11-week-old *SHIP1*$^{-/el20}$ lungs. (G) Improved survival of *SHIP1*$^{-/el20}$ mice compared with *SHIP1*$^{el20/el20}$ mice. Results for all other mice reproduced from Figure 2C. ***$P < .0001$ using log-rank (Mantel Cox) test. NS indicates not significant.

Second, we show that s-SHIP is expressed in *SHIP1*$^{-/-}$ BMMΦs but not *SHIP1*$^{el20/el20}$ BMMΦs. Third, by generating compound heterozygous *SHIP1*$^{-/el20}$ mice, we show that expression of s-SHIP rescues the *SHIP1*$^{el20/el20}$ phenotype back to the *SHIP1*$^{-/-}$ phenotype, providing genetic evidence that concomitant loss of SHIP1 and s-SHIP is the most likely explanation for the more severe phenotype. This provides the first evidence for a functional role of s-SHIP in adult hematopoiesis.

Once we identified the mutation in the *SHIP1* allele, we did not sequence the other 22 genes within the 3-Mb interval. Therefore, we cannot completely exclude the possibility that the more severe phenotype is the result of a combination of the *SHIP1*^{el20} mutation plus an independent mutation in one of the other 22 genes. However, this appears unlikely because extensive molecular studies by multiple groups indicate that, at the dose used, ENU induces single base pair changes at a rate of 1 per 1 to 2 Mb.[38] Given that the coding region of the 22 other genes is only 56 kb, the chances of additional coding sequence mutations would be extremely small.

Overall, the functions of s-SHIP appear to be synergistic with SHIP1 because the phenotype of *SHIP1*$^{el20/el20}$ mice is similar but more severe and occurs at an earlier age than *SHIP1*$^{-/-}$ mice. The major differences between *SHIP1*$^{el20/el20}$ and *SHIP1*$^{-/-}$ mice are shortened survival, marked reductions in B and T cells, and higher levels of circulating IL-6. *SHIP1*$^{el20/el20}$ mice with identical genetic background and housed in the same environment as *SHIP1*$^{-/-}$ mice develop an identical lung phenotype but at a much earlier age. The

lung infiltrate of *SHIP1*$^{-/-}$ mice has been attributed to an activated macrophage phenotype.[2,3] It is likely that the more severe lung phenotype of *SHIP1*$^{el20/el20}$ mice reflects increased macrophage activation, as demonstrated by increased serum IL-6 levels compared with age-matched *SHIP1*$^{-/-}$ mice. The impaired survival of mice lacking SHIP1 has been attributed to an inflammatory infiltrate of the lungs, although inflammation of other organs, such as the bowel, may contribute to the runting phenotype seen in *SHIP1*$^{el20/el20}$ mice.[39] Therefore, it appears likely that s-SHIP functions synergistically with SHIP1 to suppress activation of macrophages.

The reduction in B and T cells in *SHIP1*$^{el20/el20}$ mice was the other major difference with *SHIP1*$^{-/-}$ mice. Determining the lineage-specific functions of s-SHIP is complicated by the inflammatory phenotype of *SHIP1*$^{el20/el20}$ mice. In the case of SHIP1, lineage-specific deletion or transplantation studies have suggested that the B-cell deficit is partly non–cell-autonomous.[14,31] Furthermore, *SHIP1*$^{-/-}$ mice generated on an IL-6-null background can partially rescue the loss of B cells.[13] Because we were unable to generate lineage-specific deletion of s-SHIP, we used a competitive transplantation assay to distinguish cell-autonomous from non–cell-autonomous effects. Although the overall phenotype, including impaired survival and lung disease, was transplantable and therefore intrinsic to the hematopoietic system, the competitive transplantation results suggested that the loss of lymphoid cells in *SHIP1*$^{el20/el20}$ mice was mediated, at least in part, by a non–cell-autonomous mechanism. Like *SHIP1*$^{-/-}$ mice, this may in part be the result of elevated inflammatory cytokines, such as IL-6, which induces apoptosis of B cells at the pre-B-cell stage of development.[40] The competitive transplantations also suggest that the concomitant loss of SHIP1 and s-SHIP does not impair HSC activity. Some, but not all, studies have suggested a role for SHIP1 in HSC function.[30,34] However, these effects on HSCs may be indirect through defects of the cell niche or osteoporosis from hyperactive osteoclasts, which may require longer to establish than the life span of *SHIP1*$^{el20/el20}$ mice.[31,41]

The biochemical functions of SHIP1 are complex.[42] Although the predominant function of SHIP1 is through its 5′-phosphatase activity to convert PtdIns(3,4,5)P_3 to PtdIns(3,4)P_2, it also has phosphatase-independent activities by interaction with key signaling intermediates through its C-terminal domain.[43,44] Given that s-SHIP has identical 5′-phosphatase and C-terminal domains, it is likely that s-SHIP has similar complex biochemical functions. Although s-SHIP lacks the SH2 domain important for membrane localization of SHIP1, it is still capable of recruitment to the cell membrane through binding of adaptor proteins, such as Grb2 to its polyproline C-terminus.[21] Our preliminary biochemical studies were unable to demonstrate any clear difference in PI3K/mTOR signaling between macrophages that lack SHIP1 with those lacking both SHIP1 and s-SHIP. This may reflect the artificial conditions of in vitro culture. Alternatively, s-SHIP may synergize with SHIP1 in other signaling pathways that regulate the inflammatory response, such as the mitogen-activated protein kinase or nuclear factor-κB pathways.[19,45,46] In support of this possibility, the human homolog of s-SHIP, SIP-110, can bind Grb2 and inhibit phosphorylation of mitogen-activated protein kinase in a phosphatase-independent manner.[47] Two possible interactions that may be impaired by loss of both SHIP1 and s-SHIP are with the Dok proteins and the Src kinases, Lyn and Hck. Mice deficient of both SHIP1 and Dok-1 have a severe phenotype very similar to *SHIP1*$^{el20/el20}$ mice with failure to thrive, shortened life span, and marked T- and B-cell loss.[48] Alternatively, loss of both SHIP1 and s-SHIP may lead to loss of function of the Src kinases Lyn and Hck, which in part require SHIP1 for their repressive functions.[49,50]

Generation of mouse mutants by ENU mutagenesis can provide new insights into gene function that are not afforded by traditional germline targeting. Study of an ENU mouse mutant of SHIP1 provides the first functional evidence that the s-SHIP isoform of the *Inpp5d* locus synergizes with SHIP1 for suppression of macrophage activation. Generation of mice lacking only the s-SHIP isoform will be required to define any nonredundant role of s-SHIP in adult hematopoiesis.

Acknowledgments

The authors thank Melanie Howell, Marc Sacco, Lan Ta, Rebecca Bowyer, Lara Mizhiritsky, and Jenny Davis for animal husbandry; Jason Corbin for blood analyses; Dean Hewish and Catherine Li for flow cytometry; and David Tarlinton for serum immunoglobulin measurements.

This work was supported by the National Health & Medical Research Council of Australia (project grant 435107; fellowships, D.J.C., S.M.J., M.L.H., M.J.M., and D.J.H.) and the Australian Research Council (QEII fellowship; B.T.K.).

Authorship

Contribution: N.Y.N.N., M.L.H., C.A.M., D.J.H., S.M.J., and D.J.C. designed research; N.Y.N.N., M.J.M., L.M.O., E.M.D., A.A.H., J.E.C., B.T.K., D.J.H., and D.J.C. performed research; D.J.H. and M.L.H. contributed critical reagents; N.Y.N.N., M.J.M., L.M.O., E.M.D., D.J.H., A.A.H., B.T.K., M.L.H., C.A.M., and D.J.C. analyzed data; and N.Y.N.N. and D.J.C. wrote the manuscript.

Conflict-of-interest disclosure: The authors declare no competing financial interests.

Correspondence: David J. Curtis, Bone Marrow Research Laboratories, Royal Melbourne Hospital, Victoria 3050, Australia; e-mail: dcurtis@wehi.edu.au.

References

1. Ooms LM, Horan KA, Rahman P, et al. The role of the inositol polyphosphate 5-phosphatases in cellular function and human disease. *Biochem J.* 2009;419(1):29-49.
2. Helgason CD, Damen JE, Rosten P, et al. Targeted disruption of SHIP leads to hemopoietic perturbations, lung pathology, and a shortened life span. *Genes Dev.* 1998;12(11):1610-1620.
3. Rauh MJ, Ho V, Pereira C, et al. SHIP represses the generation of alternatively activated macrophages. *Immunity.* 2005;23(4):361-374.
4. Liu Q, Sasaki T, Kozieradzki I, et al. SHIP is a negative regulator of growth factor receptor-mediated PKB/Akt activation and myeloid cell survival. *Genes Dev.* 1999;13(7):786-791.
5. Sly LM, Rauh MJ, Kalesnikoff J, Song CH, Krystal G. LPS-induced upregulation of SHIP is essential for endotoxin tolerance. *Immunity.* 2004;21(2):227-239.
6. Collazo MM, Wood D, Paraiso KH, et al. SHIP limits immunoregulatory capacity in the T-cell compartment. *Blood.* 2009;113(13):2934-2944.
7. Kuroda E, Ho V, Ruschmann J, et al. SHIP represses the generation of IL-3-induced M2 macrophages by inhibiting IL-4 production from basophils. *J Immunol.* 2009;183(6):3652-3660.
8. Paraiso KH, Ghansah T, Costello A, Engelman RW, Kerr WG. Induced SHIP deficiency expands myeloid regulatory cells and abrogates graft-versus-host disease. *J Immunol.* 2007;178(5):2893-2900.
9. Wang JW, Howson JM, Ghansah T, et al. Influence of SHIP on the NK repertoire and allogeneic bone marrow transplantation. *Science.* 2002;295(5562):2094-2097.
10. Haddon DJ, Antignano F, Hughes MR, et al.

SHIP1 is a repressor of mast cell hyperplasia, cytokine production, and allergic inflammation in vivo. *J Immunol.* 2009;183(1):228-236.

11. Huber M, Helgason CD, Damen JE, Liu L, Humphries RK, Krystal G. The src homology 2-containing inositol phosphatase (SHIP) is the gatekeeper of mast cell degranulation. *Proc Natl Acad Sci U S A.* 1998;95(19):11330-11335.
12. Liu Q, Oliveira-Dos-Santos AJ, Mariathasan S, et al. The inositol polyphosphate 5-phosphatase ship is a crucial negative regulator of B cell antigen receptor signaling. *J Exp Med.* 1998;188(7): 1333-1342.
13. Maeda K, Baba Y, Nagai Y, et al. IL-6 blocks a discrete early step in lymphopoiesis. *Blood.* 2005; 106(3):879-885.
14. Karlsson MC, Guinamard R, Bolland S, Sankala M, Steinman RM, Ravetch JV. Macrophages control the retention and trafficking of B lymphocytes in the splenic marginal zone. *J Exp Med.* 2003; 198(2):333-340.
15. Tarasenko T, Kole HK, Chi AW, Mentink-Kane MM, Wynn TA, Bolland S. T cell-specific deletion of the inositol phosphatase SHIP reveals its role in regulating Th1/Th2 and cytotoxic responses. *Proc Natl Acad Sci U S A.* 2007;104(27):11382-11387.
16. Damen JE, Liu L, Rosten P, et al. The 145-kDa protein induced to associate with Shc by multiple cytokines is an inositol tetraphosphate and phosphatidylinositol 3,4,5-triphosphate 5-phosphatase. *Proc Natl Acad Sci U S A.* 1996;93(4):1689-1693.
17. Tamir I, Stolpa JC, Helgason CD, et al. The RasGAP-binding protein p62dok is a mediator of inhibitory FcgammaRIIB signals in B cells. *Immunity.* 2000;12(3):347-358.
18. Tridandapani S, Pradhan M, LaDine JR, Garber S, Anderson CL, Coggeshall KM. Protein interactions of Src homology 2 (SH2) domain-containing inositol phosphatase (SHIP): association with Shc displaces SHIP from FcgammaRIIb in B cells. *J Immunol.* 1999;162(3):1408-1414.
19. An H, Xu H, Zhang M, et al. Src homology 2 domain-containing inositol-5-phosphatase 1 (SHIP1) negatively regulates TLR4-mediated LPS response primarily through a phosphatase activity- and PI-3K-independent mechanism. *Blood.* 2005;105(12):4685-4692.
20. Ganesan LP, Joshi T, Fang H, et al. FcgammaR-induced production of superoxide and inflammatory cytokines is differentially regulated by SHIP through its influence on PI3K and/or Ras/Erk pathways. *Blood.* 2006;108(2):718-725.
21. Tu Z, Ninos JM, Ma Z, et al. Embryonic and hematopoietic stem cells express a novel SH2-containing inositol 5′-phosphatase isoform that partners with the Grb2 adapter protein. *Blood.* 2001; 98(7):2028-2038.
22. Rohrschneider LR, Custodio JM, Anderson TA, Miller CP, Gu H. The intron 5/6 promoter region of the ship1 gene regulates expression in stem/progenitor cells of the mouse embryo. *Dev Biol.* 2005;283(2):503-521.
23. Bai L, Rohrschneider LR. s-SHIP promoter expression marks activated stem cells in developing mouse mammary tissue. *Genes Dev.* 2010; 24(17):1882-1892.
24. Sly LM, Rauh MJ, Kalesnikoff J, Buchse T, Krystal G. SHIP, SHIP2, and PTEN activities are regulated in vivo by modulation of their protein levels: SHIP is up-regulated in macrophages and mast cells by lipopolysaccharide. *Exp Hematol.* 2003;31(12): 1170-1181.
25. Desponts C, Ninos JM, Kerr WG. s-SHIP associates with receptor complexes essential for pluripotent stem cell growth and survival. *Stem Cells Dev.* 2006;15(5):641-646.
26. Smyth I, Hacking DF, Hilton AA, et al. A mouse model of harlequin ichthyosis delineates a key role for Abca12 in lipid homeostasis. *PLoS Genet.* 2008;4(9):e1000192.
27. Ooms LM, Dyson JM, Kong AM, Mitchell CA. Analysis of phosphatidylinositol 3,4,5 trisphosphate 5-phosphatase activity by in vitro and in vivo assays. *Methods Mol Biol.* 2009;462:223-239.
28. Brauweiler A, Tamir I, Dal Porto J, et al. Differential regulation of B cell development, activation, and death by the src homology 2 domain-containing 5′ inositol phosphatase (SHIP). *J Exp Med.* 2000;191(9):1545-1554.
29. Helgason CD, Kalberer CP, Damen JE, et al. A dual role for Src homology 2 domain-containing inositol-5-phosphatase (SHIP) in immunity: aberrant development and enhanced function of b lymphocytes in ship −/− mice. *J Exp Med.* 2000;191(5):781-794.
30. Desponts C, Hazen AL, Paraiso KH, Kerr WG. SHIP deficiency enhances HSC proliferation and survival but compromises homing and repopulation. *Blood.* 2006;107(11):4338-4345.
31. Hazen AL, Smith MJ, Desponts C, Winter O, Moser K, Kerr WG. SHIP is required for a functional hematopoietic stem cell niche. *Blood.* 2009; 113(13):2924-2933.
32. Liu Q, Shalaby F, Jones J, Bouchard D, Dumont DJ. The SH2-containing inositol polyphosphate 5-phosphatase, ship, is expressed during hematopoiesis and spermatogenesis. *Blood.* 1998; 91(8):2753-2759.
33. Maus UA, Janzen S, Wall G, et al. Resident alveolar macrophages are replaced by recruited monocytes in response to endotoxin-induced lung inflammation. *Am J Respir Cell Mol Biol.* 2006;35(2):227-235.
34. Helgason CD, Antonchuk J, Bodner C, Humphries RK. Homeostasis and regeneration of the hematopoietic stem cell pool are altered in SHIP-deficient mice. *Blood.* 2003;102(10):3541-3547.
35. Nakamura K, Kouro T, Kincade PW, Malykhin A, Maeda K, Coggeshall KM. Src homology 2-containing 5-inositol phosphatase (SHIP) suppresses an early stage of lymphoid cell development through elevated interleukin-6 production by myeloid cells in bone marrow. *J Exp Med.* 2004; 199(2):243-254.
36. Maeda K, Mehta H, Drevets DA, Coggeshall KM. IL-6 increases B-cell IgG production in a feed-forward proinflammatory mechanism to skew hematopoiesis and elevate myeloid production. *Blood.* 2010;115(23):4699-4706.
37. Fang H, Pengal RA, Cao X, et al. Lipopolysaccharide-induced macrophage inflammatory response is regulated by SHIP. *J Immunol.* 2004; 173(1):360-366.
38. Coghill EL, Hugill A, Parkinson N, et al. A gene-driven approach to the identification of ENU mutants in the mouse. *Nat Genet.* 2002;30(3):255-256.
39. Kerr WG, Park MY, Maubert M, Engelman RW. SHIP deficiency causes Crohn's disease-like ileitis. *Gut.* 2011;60(2):177-188.
40. Nagasawa T. Microenvironmental niches in the bone marrow required for B-cell development. *Nat Rev Immunol.* 2006;6(2):107-116.
41. Takeshita S, Namba N, Zhao JJ, et al. SHIP-deficient mice are severely osteoporotic due to increased numbers of hyper-resorptive osteoclasts. *Nat Med.* 2002;8(9):943-949.
42. Kerr WG. Inhibitor and activator: dual functions for SHIP in immunity and cancer. *Ann N Y Acad Sci.* 2011;1217:1-17.
43. Wahle JA, Paraiso KH, Kendig RD, et al. Inappropriate recruitment and activity by the Src homology region 2 domain-containing phosphatase 1 (SHP1) is responsible for receptor dominance in the SHIP-deficient NK cell. *J Immunol.* 2007; 179(12):8009-8015.
44. Peng Q, Malhotra S, Torchia JA, Kerr WG, Coggeshall KM, Humphrey MB. TREM2- and DAP12-dependent activation of PI3K requires DAP10 and is inhibited by SHIP1. *Sci Signal.* 2010;3(122):ra38.
45. Kalesnikoff J, Baur N, Leitges M, et al. SHIP negatively regulates IgE + antigen-induced IL-6 production in mast cells by inhibiting NF-kappa B activity. *J Immunol.* 2002;168(9):4737-4746.
46. Gloire G, Charlier E, Rahmouni S, et al. Restoration of SHIP-1 activity in human leukemic cells modifies NF-kappaB activation pathway and cellular survival upon oxidative stress. *Oncogene.* 2006;25(40):5485-5494.
47. Deuter-Reinhard M, Apell G, Pot D, Klippel A, Williams LT, Kavanaugh WM. SIP/SHIP inhibits Xenopus oocyte maturation induced by insulin and phosphatidylinositol 3-kinase. *Mol Cell Biol.* 1997;17(5):2559-2565.
48. Kashiwada M, Cattoretti G, McKeag L, et al. Downstream of tyrosine kinases-1 and Src homology 2-containing inositol 5′-phosphatase are required for regulation of CD4+CD25+ T cell development. *J Immunol.* 2006;176(7):3958-3965.
49. Harder KW, Quilici C, Naik E, et al. Perturbed myelo/erythropoiesis in Lyn-deficient mice is similar to that in mice lacking the inhibitory phosphatases SHP-1 and SHIP-1. *Blood.* 2004;104(13): 3901-3910.
50. Xiao W, Hong H, Kawakami Y, Lowell CA, Kawakami T. Regulation of myeloproliferation and M2 macrophage programming in mice by Lyn/Hck, SHIP, and Stat5. *J Clin Invest.* 2008;118(3): 924-934.